

Article

# Sustainable Solvent-Free Selective Oxidation of Benzyl Alcohol Using Ru(0) Supported on Alumina

Eleonora Aneggi <sup>1,\*</sup>, Filippo Campagnolo <sup>1</sup>, Daniele Zuccaccia <sup>1</sup>, Walter Baratta <sup>1</sup>, Jordi Llorca <sup>2</sup>  
and Alessandro Trovarelli <sup>3</sup>

<sup>1</sup> Department of Agricultural, Food, Environmental and Animal Sciences, Section of Chemistry, University of Udine, INSTM Udine Research Unit, 33100 Udine, Italy

<sup>2</sup> Institute of Energy Technologies, Department of Chemical Engineering and Barcelona Research Center in Multiscale Science and Engineering, Universitat Politècnica de Catalunya, 08019 Barcelona, Spain

<sup>3</sup> Polytechnic Department of Engineering and Architecture, University of Udine, INSTM Udine Research Unit, 33100 Udine, Italy

\* Correspondence: [eleonora.aneggi@uniud.it](mailto:eleonora.aneggi@uniud.it); Tel.: +39-0432558840

**Abstract:** The selective oxidation of primary alcohols into their corresponding carbonyl compounds is challenging because of the easy over oxidation to acids and esters. The traditional reaction requires large amounts of solvent and oxidant, causing serious environmental issues. Recently, several efforts have been made to transform the reaction into a more sustainable process. Here, we investigated the solvent-free oxidation of benzyl alcohol using air as a green oxidant in the presence of ruthenium supported on alumina and zirconia, thereby meeting atom economy and environmental requirements. The materials were extensively characterized and, in addition to their activity, selectivity, and reusability, the environmental sustainability of the process was assessed according to green chemistry metrics. XRD, TEM, and XPS analyses suggest that the formation of metallic Ru on the support plays a key role in the catalytic activity. Ru supported on alumina, after a reduction treatment, achieves good activity (62% conversion) and a complete selectivity in a very sustainable process (without a solvent and with air as oxidant), as indicated by the very low E-factor value. The formulation is very stable and maintains high activity after recycling.

**Keywords:** ruthenium; heterogeneous catalysis; selective oxidation; sustainable process; E-factor; benzyl alcohol



**Citation:** Aneggi, E.; Campagnolo, F.; Zuccaccia, D.; Baratta, W.; Llorca, J.; Trovarelli, A. Sustainable Solvent-Free Selective Oxidation of Benzyl Alcohol Using Ru(0) Supported on Alumina. *Inorganics* **2023**, *11*, 177. <https://doi.org/10.3390/inorganics11050177>

Academic Editor: Antonino Gulino

Received: 28 February 2023

Revised: 7 April 2023

Accepted: 20 April 2023

Published: 22 April 2023



**Copyright:** © 2023 by the authors. Licensee MDPI, Basel, Switzerland. This article is an open access article distributed under the terms and conditions of the Creative Commons Attribution (CC BY) license (<https://creativecommons.org/licenses/by/4.0/>).

## 1. Introduction

Selective oxidation is a crucial process in the chemical industry due to the extensive use of the produced intermediates as precursors of fine chemicals (e.g., fragrances, drugs, and vitamins) [1–5]. Benzaldehyde is a precursor of several derivatives in the pharmaceutical and agricultural industries, and its production from benzyl alcohol has been extensively investigated [1,2,6,7]. Recently, heterogeneous catalysts have been proposed as substitutes for use in homogeneous reactions [8–10] because they can be separated and recycled more easily [4].

Specifically, the selective oxidation of alcohols into their corresponding carbonyl compounds is challenging for several reasons. The first problem is selectivity due to the ease by which aldehydes can be over oxidized into their corresponding acids and esters when primary alcohols are used. Secondly, the classical oxidation reaction is not environmentally friendly as it is carried out using organic solvents such as toluene, acetonitrile, and others [11–13]. In addition, it uses non-green stoichiometric oxidants, such as permanganate, chromate, organic peroxides, etc. [14–16], thus increasing the amount of harmful waste and environmental pollution. Over the years, various heterogeneous metal-based catalysts (Pd, Pt, Au, etc.) have been proposed for the selective oxidation of benzyl alcohol, but reactions are usually carried out in an excess of solvent and with a strong oxidant [1,3,4,14,15,17–22].

In recent decades, much attention has been paid to the sustainability of chemical reactions and, from this point of view, attempts have been made to modify traditional syntheses by favoring reactions in milder conditions, in the absence of solvents, and with greener oxidants [1–3,16,19]. Concerning the oxidation of alcohol, particular attention is being paid to the development of clean procedures that can save energy (mild conditions) and solvents (solvent-free reactions or reactions using green solvents), and that can use molecular oxygen, a greener, cheaper, and safer oxidant.

Ru-based catalysts are promising materials that may be used in several oxidation reactions [23–30], and they have shown interesting activity in the selective oxidation of alcohols. Several compositions have been investigated [31–36], and among these the effectiveness of Ru/Al<sub>2</sub>O<sub>3</sub> in the oxidation of activated and non-activated alcohols has been demonstrated by Yamaguchi et al. [37], while Zhao et al. have developed a very efficient process involving colloidal Ru nanoparticles [38]. The role of ruthenium is strictly dependent on the nature of the support, the oxidation state of the Ru, and its particle size [38–41]. In previous work [42], we investigated the catalytic activity of ruthenium supported on ceria-based materials for the selective oxidation of benzyl alcohol into benzaldehyde. The activity was mainly related to the strong interaction between RuO<sub>2</sub> and the reducible support, and the formation of highly mobile oxygen species. Ru supported on ceria-zirconia is very active, but it undergoes a progressive decrease in conversion after several reaction cycles. Here, we would like to study ruthenium supported on a different class of high-surface area metal oxides, i.e., “non-reducible oxides” such as zirconia and alumina. Despite the great interest in Ru-based formulations for the selective oxidation of alcohols, to the best of our knowledge, this is the first application of Ru supported on Al<sub>2</sub>O<sub>3</sub> for solvent-free reactions. The investigated materials were characterized and the differences in activity were rationalized in terms of the high dispersion of metallic ruthenium nanoparticles on the alumina support. Particular attention was paid to the recyclability of the most promising formulation.

The main goal of this work is to achieve a more sustainable process, and for this reason, in addition to the activity, selectivity, and reusability of the proposed formulations, the environmental acceptability of the reaction was evaluated using green chemistry metrics.

In recent decades, the attention paid to the sustainability of processes has grown considerably, and indicators have been developed to evaluate the sustainability of a reaction [43–47]. In the general evaluation of a chemical process, therefore, parameters such as the use of solvents and harmful reagents, the production of waste, and energy consumption are considered. Over the years, numerous indicators have been developed to compare the sustainability of processes, and among these, the *E-factor* and mass productivity (*MP*) play an important role [48–50]. The *E-factor* is related to the amount of waste produced for a given mass of a desired product (Equation (1)). Its evaluation is essential for minimizing waste and improving resource efficiency; the lower the value, the lower the amount of waste produced [43,51].

$$E - factor = \frac{mass\ waste}{mass\ of\ desired\ product} \quad (1)$$

A second metric that is very useful in this kind of evaluation is mass productivity. In this case, all the materials used in the process are taken into consideration (reagents, solvents, catalysts, etc.) [49,51]. *MP* is the percentage ratio between the mass of the desired product and the total mass of the materials used (Equation (2)).

$$MP\ (\%) = \frac{mass\ of\ desired\ product \times 100}{total\ mass\ of\ used\ materials} \quad (2)$$

Here, we assessed the sustainability of the proposed reaction using *E-factor* and *MP*. Ruthenium supported on alumina shows a good activity, a complete selectivity, and promising environmental sustainability.

## 2. Results and Discussion

Two different high-surface area samples modified with Ru were investigated as catalysts for the solvent-free selective oxidation of benzyl alcohol with air. The composition and BET surface area of the investigated materials are reported in Table 1. Adsorption isotherms are shown in Figure S1. The zirconia had a surface area of 64 m<sup>2</sup>/g, while the alumina had higher surface area (around 180 m<sup>2</sup>/g). After impregnation, for both supports, the surface area showed a slight decrease. The crystallite size obtained according to the Scherrer equation was not affected by the impregnation of ruthenium salt and was around 14 nm for the Zr formulations and 10 nm for the alumina materials.

**Table 1.** Composition, textural characterization, and hydrogen consumption in H<sub>2</sub>-TPR (temperature-programmed reduction experiment) profiles in the 50–200 °C region of the investigated samples.

Name	Composition	Surface Area (m <sup>2</sup> /g)	Crystallite Size (nm) <sup>a</sup>	mmol H <sub>2</sub> /g
Al	Al <sub>2</sub> O <sub>3</sub>	184	10	/
AlRu	2%Ru/Al <sub>2</sub> O <sub>3</sub>	176	10	0.37
AlRu-R <sup>b</sup>	2%Ru/Al <sub>2</sub> O <sub>3</sub>	175	10	/
Zr	ZrO <sub>2</sub>	64	14	/
ZrRu	2%Ru/ZrO <sub>2</sub>	58	14	0.22
ZrRu-R <sup>b</sup>	2%Ru/ZrO <sub>2</sub>	58	14	/

<sup>a</sup>: calculated with Scherrer formula from X-ray diffraction patterns. <sup>b</sup>: after reduction at 300 °C for 2 h under 100 mL/min of 50% H<sub>2</sub>/N<sub>2</sub> gas mixture.

The structural characteristics of zirconia- and alumina-based materials were investigated using x-ray diffraction (XRD) measurements (Figure 1).

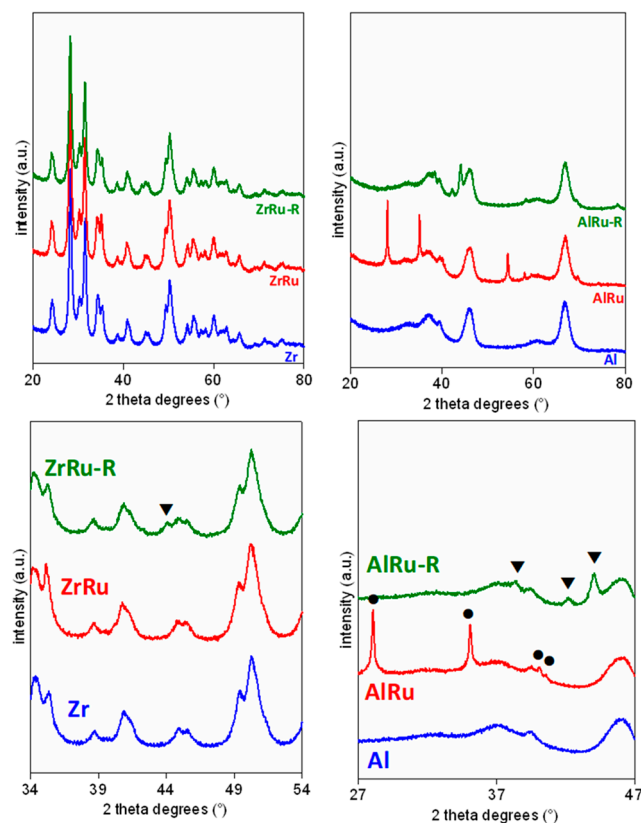


**Figure 1.** XRD profiles of (left) ZrO<sub>2</sub>- and (right) Al<sub>2</sub>O<sub>3</sub>-based catalysts. At the bottom, magnified zones are shown to highlight peaks belonging to Ru and RuO<sub>2</sub> (▼, Ru; ●RuO<sub>2</sub>).

For all the materials, the peaks belonging to the support are clearly observable. For the zirconia catalyst, the  $\text{RuO}_2$  peaks are not visible because the  $\text{ZrO}_2$  peaks are superimposed, while for the AlRu, the ruthenium oxide peaks are very well defined ( $2\theta = 28.1, 35.1, 40.1, 40.7,$  and  $54.5^\circ$ ). The XRD profiles confirm the reduction of  $\text{RuO}_2$  to metallic Ru after treatment in  $\text{H}_2/\text{N}_2$ . Indeed, a very low signal can be observed at  $2\theta = 44^\circ$  in the ZrRu-R due to the Ru. The presence of metallic Ru is better defined in the AlRu-R sample, with peaks at  $2\theta = 38.4, 42.2,$  and  $44^\circ$ .

The reducibility of the materials was also investigated using  $\text{H}_2$ -temperature-programmed reduction (Figure 2). The Zr and Al supports exhibited a flat signal, a conventional TPR profile of “non reducible” materials. After the addition of the Ru, the TPR profiles showed a low temperature peak, attributable to the reduction of  $\text{RuO}_2$ , at around  $115^\circ\text{C}$  for the AlRu and around  $140^\circ\text{C}$  for the ZrRu. After reduction, the ZrRu-R and AlRu-R showed only two negligible peaks (at around  $150^\circ\text{C}$  and  $310^\circ\text{C}$ ), which could be related to the support or to some residual  $\text{RuO}_2$ . The TPR measurements confirmed the formation of  $\text{RuO}_2$  in the prepared materials and its subsequent transformation into metallic Ru after reduction treatment. A quantitative analysis of the TPR profile in the  $50\text{--}200^\circ\text{C}$  region (Table 1) for the ZrRu and AlRu indicated a partial reduction of  $\text{RuO}_2$  for the ZrRu ( $0.22\text{ mmol/g}_{\text{cat}}$ ) and an almost complete reduction for the AlRu ( $0.37\text{ mmol/g}_{\text{cat}}$ ) when compared with the calculated amount of hydrogen consumption required for the complete reduction of  $\text{RuO}_2$  ( $0.39\text{ mmol/g}_{\text{cat}}$ ).

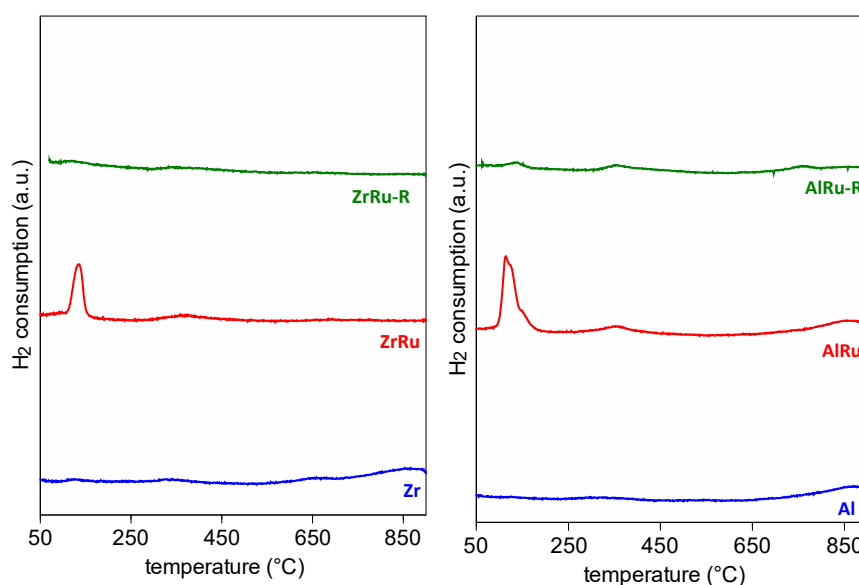


**Figure 2.**  $\text{H}_2$ -TPR profiles of investigated samples.

Figure 3 and Table S1 show the oxidation results for benzyl alcohol to benzaldehyde in the presence of the alumina- and zirconia-based formulations under air at  $90^\circ\text{C}$  for 24 h. Preliminary tests without a catalyst and over bare supports did not result in any oxidation into benzaldehyde, indicating that bare alumina and zirconia oxides are not active in this temperature range. Furthermore, these results indicate that benzyl alcohol does not have an adsorption effect on the support surface. When ruthenium was added to the support, an increase in the benzaldehyde yield was observed. For all the Ru-based materials, the selectivity to benzaldehyde was complete. The prepared catalysts were only moderately active after 24 h in the oxidation of benzyl alcohol, with a 10% and 21% conversion for the AlRu and ZrRu, respectively. When the reaction was carried out using reduced materials, a higher conversion was obtained, with remarkable results for the AlRu-R (62%). For both the supports, the conversion reached a maximum when the ruthenium was in a metallic state, and when the  $\text{RuO}_2$  was formed on the surface, the conversion was lower.

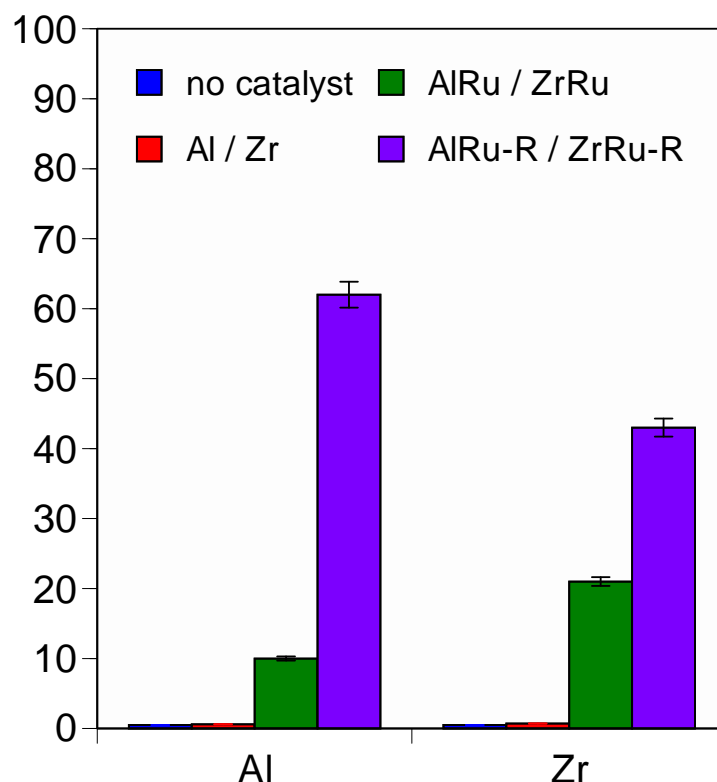


**Figure 3.** Selective conversion of benzyl alcohol to benzaldehyde (reaction conditions: 1 mL of benzyl alcohol, 200 mg of catalyst, 90 °C for 24 h, 10 mg of hexamethylbenzene as internal standard).

In order to better elucidate the differences in catalytic activity, further characterization was carried out. Specifically, X-ray photoelectron spectroscopy measurements and transmission electron microscopy measurements were obtained.

XPS was performed to better investigate the Ru oxidation state in the prepared materials (Table 2). The chemical state of the surface Ru was analyzed by means of the Ru 3d<sub>5/2</sub> signal to avoid overlapping with the C 1s signal. The ZrRu and AlRu displayed one peak at 280.8 eV that could be assigned to the Ru<sup>4+</sup> species, indicating that the Ru was mainly in the oxidized state (RuO<sub>2</sub>) [30]. The in situ-treatment under the H<sub>2</sub> atmosphere induced a change in the chemical state of the surface ruthenium. Indeed, peaks due to RuO<sub>2</sub> disappeared, and signals at 280.1 eV and 280.0 eV, due to the metallic Ru species, were identified in the ZrRu-R and AlRu-R, respectively (Figure S2). For both the supports, the initial ruthenium oxide was converted into a metallic state during the reduction treatment. These results are in agreement with the XRD and H<sub>2</sub>-TPR analyses. It is important to observe that metallic ruthenium is stable and it is not oxidized back to RuO<sub>2</sub> when exposed to air, as was confirmed by the fact that the metallic Ru peaks were found in the XRD patterns of the reduced samples that were recorded under an air atmosphere.

**Table 2.** XPS results of materials as prepared and after in situ reduction with H<sub>2</sub>/Ar at 300 °C for 1 h.

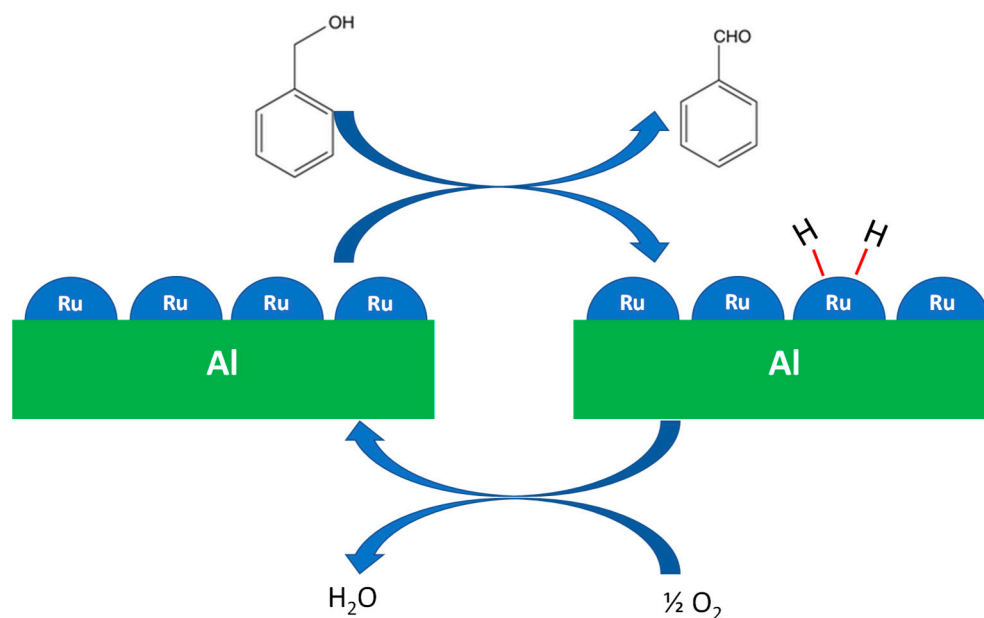
Sample	Ru/(Zr + Al) % Atomic	Ru 3d <sub>5/2</sub> eV
ZrRu	0.020	280.8 (RuO <sub>2</sub> )
ZrRu-R	0.022	280.1 (Ru)
AlRu	0.011	280.8 (RuO <sub>2</sub> )
AlRu-R	0.036	280.0 (Ru)

The Ru dispersion for the investigated formulations was estimated from the signal ratio between the Ru and the Zr or Al. The Zr-based samples showed a rather stable

dispersion before and after the reduction treatment (0.020 and 0.022, respectively), while for the Al-based materials, the dispersion significantly increased after the in situ reduction (0.011 versus 0.036). The activity seems to have been strictly related to the dispersion of the Ru species ( $\text{RuO}_2$  or Ru) on the support surface (Figure S3). For similar surface Ru dispersion values, the catalytic activity is significantly higher when the ruthenium is in a metallic state (43%) with respect to the oxide (20%). Under the conditions of the alcohol oxidation experiment, the catalytic activity was mainly due to the presence of metallic ruthenium rather than  $\text{RuO}_2$ .

Similar results were obtained by Grunwaldt et al. for Pd/ $\text{Al}_2\text{O}_3$  catalysts in the selective oxidation of alcohols [52]; the Pd supported formulations were more active after reduction than before reduction. Ruthenium supported on alumina exhibits opposite behavior compared with Ru supported on ceria-based oxides. In fact, in the case of supports based on reducible oxides, ruthenium oxide favors their activity. In this regard, it is important to remember the important role that metal–support interactions can have on a reaction. Weak metal–support interactions are usually found in cases of metal nanoparticles dispersed on non-reducible supports, whereas strong metal–support interactions occur for reducible oxides [53]. The different metal–support interactions that occur between Ru/ $\text{Al}_2\text{O}_3$  and Ru/ $\text{CeZrO}_2$  affect the active form of the metal and its activity. When ruthenium is deposited on ceria-based oxides,  $\text{Ru}^{\text{III}}$  species, such as  $\text{RuO}_2$ , can easily interact with the support, increasing the concentration of oxygen vacancies [42,53]. In several oxidation reactions, it has been observed that, when Ru is supported on “non-reducible” oxides, the activity of metallic ruthenium is higher than that of  $\text{RuO}_2$  [54–59].

In summary, metallic Ru on AlRu-R shows higher activity in the oxidation of benzyl alcohol, while  $\text{RuO}_2$  in AlRu is much less active. This suggests that the oxidation of the alcohol occurs by a dehydrogenation mechanism (as is proposed in Scheme 1) similar to what was obtained by Grunwaldt et al. with metallic Pd [52]. The proposed mechanism is initiated by the dehydrogenation of the alcohol, the formation of the aldehyde, and the adsorption of hydrogen on metallic Ru. The molecular oxygen then removes the hydrogen from the Ru.



**Scheme 1.** Overall reaction of oxidation on metallic Ru.

The stability of AlRu-R was investigated for several repeated reaction cycles, and no significant change in conversion was observed after three cycles (Figure 4).

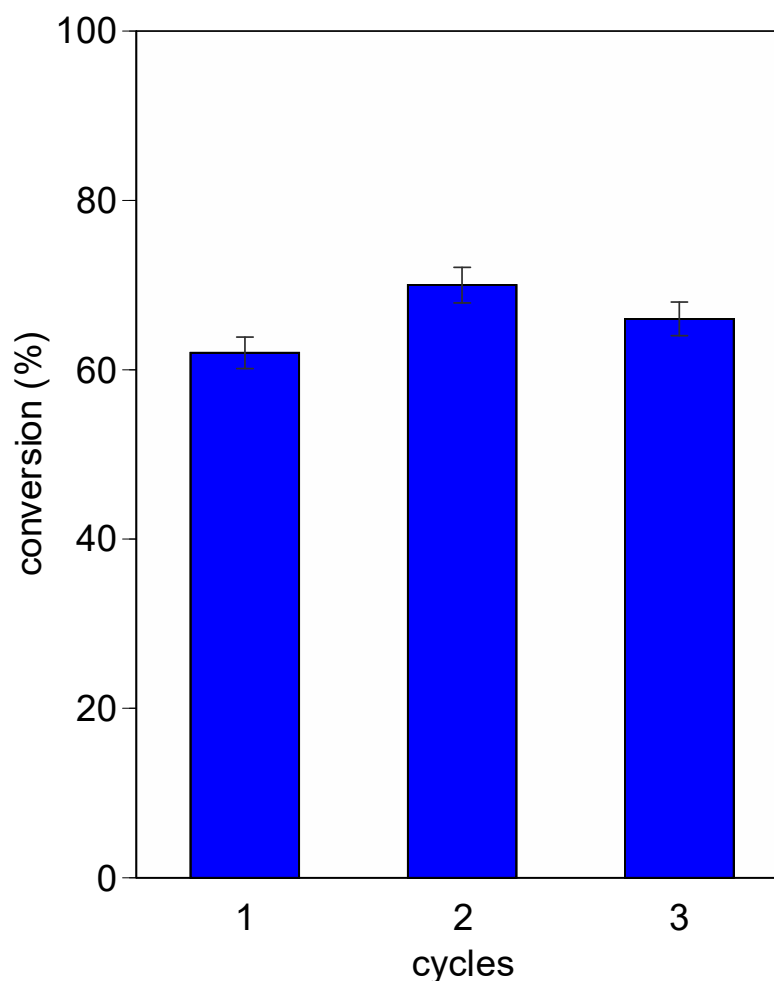


**Figure 4.** Reusability of AlRu-R (selectivity is 100%). Reaction conditions: 1 mL of benzyl alcohol, 200 mg of catalyst, 90 °C for 24 h, 10 mg of hexamethylbenzene as internal standard.

Because of the higher activity of ruthenium supported on alumina compared with zirconia-based catalysts, STEM-HAADF and HRTEM analyses were carried out to further investigate the materials. Specifically, these observations can highlight variations in the morphology and size of the prepared materials and the reduced alumina-based samples.

Figure 5A shows a STEM-HAADF image of the AlRu. Bright particles of about 12 nm in size are recognizable (see red arrow). A STEM-HAADF image recorded at a higher magnification is shown in Figure 5B. Three bright particles are seen in the upper left part of the image. An EDX spectrum recorded in the area enclosed by the red circle is included. In addition to the Al and O signals originating from the alumina support, Ru peaks are also recorded, indicating that the bright particles contain Ru. High-resolution TEM images (HRTEM) are shown in Figure 5C,D. In Figure 5C, the alumina support particles show lattice fringes at 4.5 Å, which correspond well to the (111) crystallographic planes of Al<sub>2</sub>O<sub>3</sub>. A Fourier transform analysis of the particle showing lattice fringes (area inside the red square) shows spots at 3.2 Å, which can be ascribed to the (110) crystallographic planes of RuO<sub>2</sub>. The circle at 2.4 Å in the FT image corresponds to the (311) planes of the alumina support nanoparticles. In Figure 5D, (311) planes of alumina at 2.4 Å are identified with low electron contrast. RuO<sub>2</sub> particles in the range 5–15 nm are recognized by their characteristic lattice spacing at 3.2 Å, corresponding to the (110) crystallographic planes.

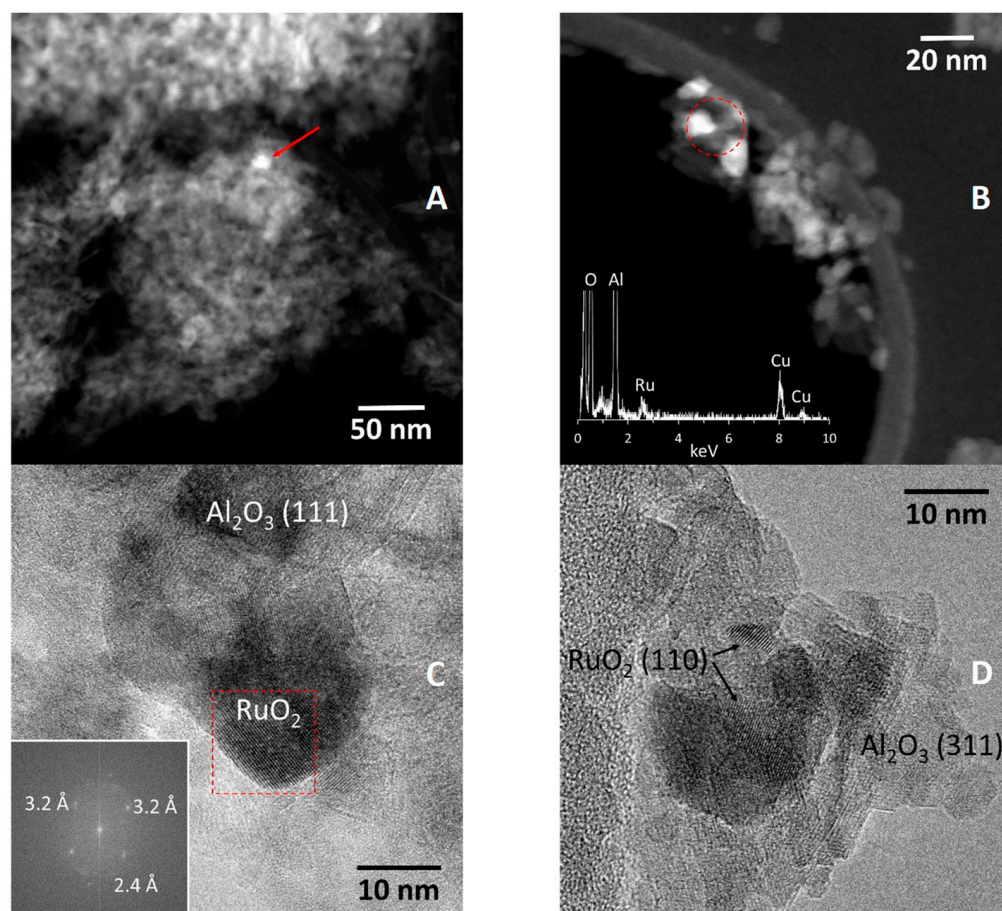


**Figure 5.** STEM-HAADF (A,B) and HRTEM (C,D) analyses of AlRu.

After reduction, the AlRu-R sample showed metal particles with different sizes. Figure 6A shows a STEM-HAADF image in which very small nanoparticles of about 1–2 nm in size (see arrows) can be seen coexisting with large particles exceeding 50 nm in size. The EDX analysis included in Figure 6A corresponds to the area enclosed in the red circle which shows one of the bright particles. A prominent Ru signal indicates that the particle is composed of Ru. Figure 6B shows an HRTEM image. Large Ru particles cannot be imaged by HRTEM because they are too thick. The image in Figure 6B shows the small Ru nanoparticles (see arrows). Given their small size (around 1 nm), it has been not possible to record lattice fringe images.

General HRTEM images of the AlRu-R after the reaction are shown in Figure 6C,D. In the HRTEM image shown in Figure 6C, several Ru nanoparticles are identified by their dark contrast. They measure about 4–8 nm. This suggests that the sintering of the 1–2 nm Ru nanoparticles seen in the sample after reduction may have occurred during the reaction. The nature of these nanoparticles was determined using HRTEM. Figure 6D shows a metallic Ru nanoparticle exhibiting lattice fringes at 1.4 Å, corresponding to the (110) crystallographic planes. The Ru nanoparticles are in close contact with the alumina support nanoparticles, identified in the image by their lattice fringes at 2.4 Å, and corresponding to the (311) crystallographic planes.

In summary, the AlRu contained RuO<sub>2</sub> nanoparticles in the 5–15 nm range, while the AlRu-R, both before and after the reaction, showed the coexistence of large Ru particles (50 nm) and small Ru nanoparticles (1–2 nm before the reaction and 4–8 after the reaction). The stability of the AlRu-R after three cycles was probably due to the presence of small crystallites of Ru, which, despite showing a tendency to sinter, remained very small (4–8 nm).

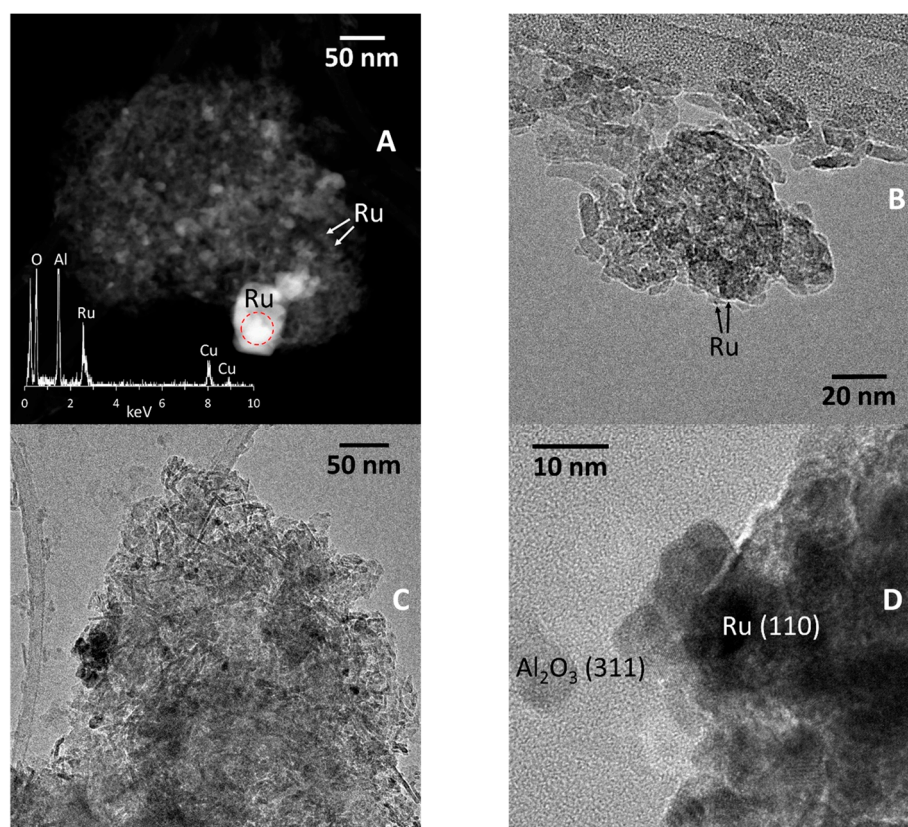


**Figure 6.** STEM-HAADF and HRTEM analyses of AlRu-R before (A,B) and after (C,D) the reaction.

The AlRu-R showed a good conversion of 62% at 90 °C. A comparison with an heterogeneous catalyst reported in literature under solvent-free conditions suggests that AlRu-R is an active heterogeneous catalyst (Table 3).

**Table 3.** Comparison of results for benzyl alcohol oxidation with heterogeneous catalyst in solvent-free reaction.

Catalyst	Catalyst (mg)	Alcohol (mmol)	O <sub>2</sub>	T (°C)	Time (h)	Conv (%)	Select (%)	Ref.
Pd/SiO <sub>2</sub> -Al <sub>2</sub> O <sub>3</sub>	100	48.5	3 mL/min	70	10	97	98	[17]
Ru	20	27.7	10 atm	100	5	93	90	[38]
Au-Pd/CeO <sub>2</sub> rod	50	144	3 atm	120	3	78	88	[21]
Pd/CN-1.0/CeO <sub>2</sub>	50	51.2	20 mL/min	90	5	77	>99	[60]
AlRu-R	200	9.6	1 atm	90	24	62	100	this study
CZRu	200	9.6	1 atm	90	24	61	100	[42]
1%Au-Pd/TiO <sub>2</sub>	20	18.5	1 atm	120	1	56	74	[19]
1%Pd-Zn/TiO <sub>2</sub>	20	18.5	1 atm	120	1	55	81	[18]
PtRu/C	100	193	10 atm	100	8	17	99	[61]
Ru/TiO <sub>2</sub>	120	96.6	1 atm	110	3	10	98	[62]

A comparison between the studies reported in Table 3 is rather difficult due to the great variability in the reaction parameters, in particular regarding the substrate/catalyst ratio, the amount of O<sub>2</sub>, and the temperature. Formulations based on Pd, Au, and their combination are widely used in the selective oxidation of alcohols. The most active catalysts (Pd/SiO<sub>2</sub>-Al<sub>2</sub>O<sub>3</sub>, Ru, Au-Pd/CeO<sub>2</sub> rod, and Pd/CN-1.0/CeO<sub>2</sub>) achieve a very high conversion (in the 77–97% range), but only when the reactions are carried out at severe conditions, e.g., under 3–10 atm of pure O<sub>2</sub> or in O<sub>2</sub> flow (3–20 mL/min), thus sustaining the process [17,21,38,60]. It is easier to compare reactions carried out at atmospheric pres-

sure. Bimetallic Pd catalysts with Au or Zn supported on  $\text{TiO}_2$  [18,19] show interesting activity (55–56%) and selectivity (74–81%), while Ru supported on C [61,62] and  $\text{TiO}_2$  shows very high selectivity but low activity (10–17%). The catalytic activity of AlRu-R developed here is comparable to that obtained with Ru supported on ceria-zirconia, a reducible material [42]. The oxidation reactions were carried out under the same reaction conditions, and consequently it is possible to make a precise comparison between the two formulations. The main difference is the nature of the support; indeed, while ceria-zirconia is a reducible material with a moderate surface area ( $80 \text{ m}^2/\text{g}$ ) and high oxygen storage capacity,  $\text{Al}_2\text{O}_3$  is a non-reducible material with a very high surface area ( $180 \text{ m}^2/\text{g}$ ). The catalytic activity is strictly correlated to the different metal–support interactions (Figure 7).

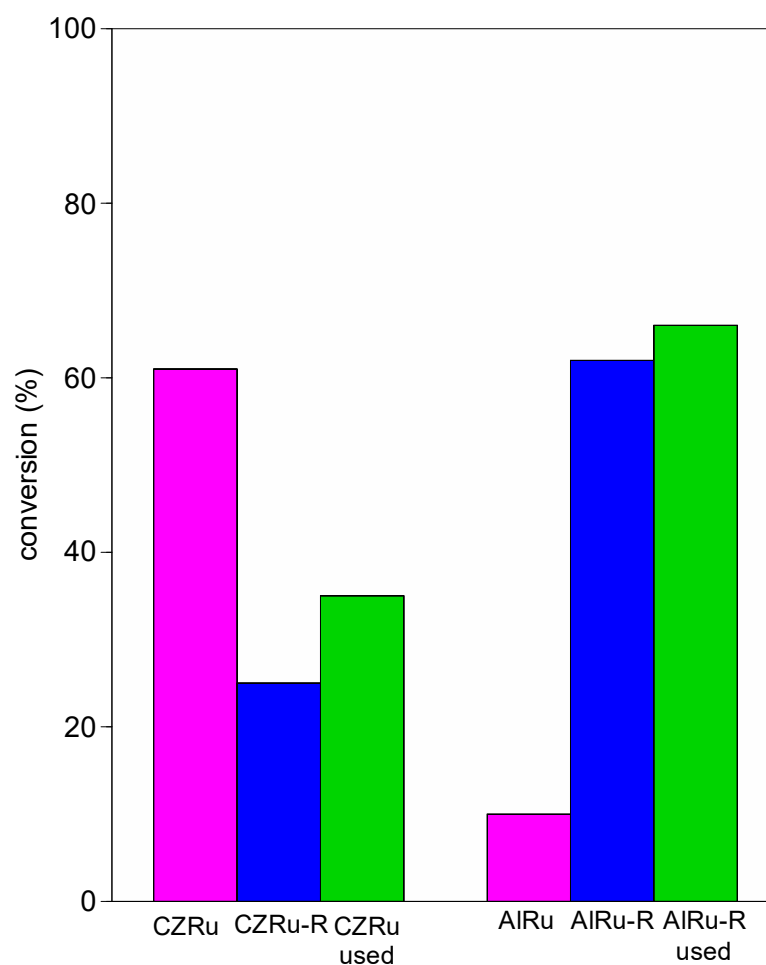


**Figure 7.** Selective conversion of benzyl alcohol to benzaldehyde for Ru supported on alumina and ceria-zirconia (reaction conditions: 1 mL of benzyl alcohol, 200 mg of catalyst,  $90^\circ\text{C}$  for 24 h, 10 mg of hexamethylbenzene as internal standard).

For the reducible ceria-zirconia, higher activity was found when the ruthenium formed  $\text{RuO}_2$  on the support surface. Indeed, the activity was strongly related to the increased mobility of the surface oxygen resulting from the close interaction of the metal oxide and the ceria-zirconia with the formation of the bridging oxygen Ru-O-Ce and the superoxide species ( $\text{O}_2^-$ ). For the non-reducible alumina support, the activity was higher when the ruthenium was in a metallic state. In this case, the activity was related to the formation of metallic Ru-species that enhanced the oxidation of the benzyl alcohol via a dehydrogenation mechanism.

A great difference in reusability was found for the two formulations. While the CZRu progressively decrease the activity, the AIRu-R was very stable after three cycles, confirming

the attractiveness of this catalyst for the solvent-free selective oxidation of benzyl alcohol to benzaldehyde.

For a better understanding of the sustainability of the process, we considered two green chemistry metrics, the E-factor and the MP (mass productivity) of the catalytic reactions from Table 3 carried out under atmospheric pressure (Figure 8). Assessing the potential environmental impact of the entire process is complicated and requires a full life cycle analysis, but this is beyond the scope of our study, which is only a preliminary investigation intended to develop an understanding of the environmental acceptability of the reaction. Therefore, here we used E-factor and mass productivity to carry out a direct comparison with other formulations used in the same type of process (neat reaction). First of all, it is important to note that the reaction temperature used for the oxidation on the AlRu-R and CZRu was lower than that used in any of the other processes, resulting in energy savings. The best sustainability results were obtained for the AlRu-R and CZRu, which achieved excellent green chemistry metrics compared with the other selected formulations, with an E-factor of less than 1 and an MP of approximately 50%. A E-factor of 0.95 is typical in the bulk chemistry sector [50]. For the AlRu-R and CZRu, green metrics were also calculated for the third recycle and, in this case, the AlRu-R shows better metrics (E-factor 0.51 and MP 66%) due to its stability over different reaction cycles. In summary, after a detailed comparison with other formulations reported in the literature, we determined that AlRu-R, as a material for use in the oxidation of benzyl alcohol, is interesting and has a low environmental impact in terms not only of conversion, selectivity, and stability, but also in terms of the sustainability of the process and the reduction of waste.

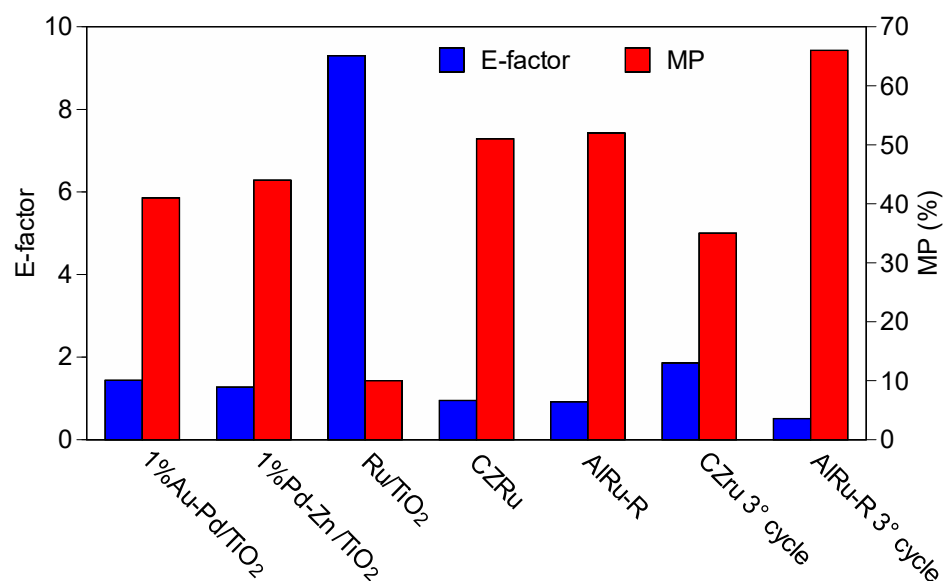


**Figure 8.** Comparison of E-factor and mass productivity (MP) of selected heterogeneous catalysts from Table 3 for benzyl alcohol oxidation.

### 3. Materials and Methods

#### 3.1. Catalyst Preparation

A sample of commercial zirconium hydroxide (Mel chemicals) was calcined at 500 °C for 3 h to obtain the zirconium oxide support. A sample of alumina (Sasol) was used as received. The materials were prepared via incipient wetness impregnation (IW) of the metal oxides with aqueous solutions of ruthenium nitrosyl nitrate (Sigma–Aldrich) in order to obtain Ru(2%)/MxO<sub>y</sub>, with MxO<sub>y</sub> = Al<sub>2</sub>O<sub>3</sub>, and ZrO<sub>2</sub>. Samples were dried overnight at 100 °C and then calcined at 500 °C for 3 h (AlRu and ZrRu). All the materials were also treated at 300 °C for 2 h under 100 mL/min of a 50% H<sub>2</sub>/N<sub>2</sub> gas mixture (reduced samples are indicated as AlRu-R and ZrRu-R).

### 3.2. Catalyst Characterization

The textural characteristics were measured according to the B.E.T. method via nitrogen adsorption at 77 K using a Tristar 3000 gas adsorption analyzer (Micromeritics, Norcross, GA, USA). The structural features of the catalysts were investigated using X-ray diffraction. The spectra were recorded on a Philips X'Pert diffractometer (equipped with a real-time multiple-strip detector) operated at 40 kV and 40 mA using Ni-filtered Cu-K $\alpha$  radiation ((PANalytical B.V., Almelo, The Netherlands). The spectra were collected using a step size of 0.02° and a counting time of 40 s per angular abscissa in the range 20°–145°. The Philips X'Pert HighScore software was used for phase identification. The mean crystalline size was estimated from the full width at the half maximum (FWHM) of the X-ray diffraction peak using the Scherrer [63].

The reducibility of the catalysts was studied via temperature-programmed reduction (TPR) experiments (Autochem II 2920 Instrument, Micromeritics, Norcross, GA, USA). The catalysts (40 mg) were heated without pretreatment at a constant rate (10 °C/min) in a U-shaped quartz reactor from room to a temperature of 900 °C under a flowing hydrogen/nitrogen mixture (35 mL/min, 4.5% H<sub>2</sub> in N<sub>2</sub>). The hydrogen consumption was monitored using a thermal conductivity detector (TCD). The quantification of the H<sub>2</sub> consumption was carried out by calibrating the signal with the introduction of known amounts of hydrogen.

X-ray photoelectron spectroscopy (XPS) was performed on a SPECS system equipped with a XR50 source operating at 250 W and a Phoibos 150 MCD-9 detector (SPECS GmbH, Berlin, Germany). The energy step of the high-resolution spectra was set at 0.05 eV. Atomic fractions were calculated using peak areas normalized on the basis of acquisition parameters after background subtraction, experimental sensitivity factors, and transmission factors provided by the manufacturer. In situ reduction treatments were carried out at 300 °C and 1 bar for 3 h under a H<sub>2</sub>:Ar = 1:1 mixture. The sample was heated with an IR lamp and the temperature was measured with a thermocouple in contact with the sample.

HRTEM and STEM-HAADF images were obtained using a field emission gun FEI Tecnai F20 microscope (FEI Company, Hillsboro, Oregon, United States) equipped with a field emission source at an accelerating voltage of 200 kV with a point-to-point resolution of 0.19 nm. The average particle diameter was calculated from the mean diameter frequency distribution using the following formula:  $d = \sum n_i d_i / \sum n_i$ , where  $n_i$  is the number of particles with a particle diameter of  $d_i$  in a certain range.

### 3.3. Alcohol Oxidation

The solvent-free oxidation of benzyl alcohol was carried out in a 5 mL round-bottom flask equipped with a condenser under continuous stirring conditions. For a typical run, 0.2 g of catalyst, 1 mL of benzyl alcohol (9.7 mmol), and 0.01 g of hexamethylbenzene (Sigma Aldrich) as the internal standard were placed in a flask and heated to 90 °C for 24 h under atmospheric pressure. In order to verify the stability of the hexamethylbenzene during the reaction, black tests were carried out in the absence of the substrate using toluene as a solvent. The spectra before and after the reaction did not show the modification or presence of any degradation products.

The progress of the reaction was checked for <sup>1</sup>H NMR using a Bruker Avance III HD (Bruker Italia Srl, Milan, Italy) 400 MHz spectrometer at 298 K equipped with carousel of 24 samples and an automation program, IconNMR, which managed the analysis from the insertion of the sample to the integration of the spectra signals. The deuterated solvent, CDCl<sub>3</sub> (Sigma Aldrich, Merk Life Science S.r.l., Milano, Italy), was used without any further purification. The reaction mixture (10  $\mu$ L) was taken with a syringe and dissolved in 500  $\mu$ L of anhydrous CDCl<sub>3</sub>. The conversion was calculated from the integral area of the singlet at 4.72 ppm, corresponding to the -CH<sub>2</sub> protons of the benzyl alcohol, and compared with the hexamethylbenzene signals (2.30 ppm) as internal references. After the reaction, a signal at 10 ppm was attributed to the proton resonance of the aldehyde group (Figure S4). The reported conversions are an average of three runs, and the resulting errors were within

3%. The selectivity was evaluated through the analysis of the products obtained after the reaction.

The recycling of the catalyst was investigated in multiple runs. After the first catalytic run, the catalyst was recovered via evaporation, dried under vacuum at 150 °C for 10 min, and then reused in the next run under the same conditions. After each recovery, a loss of about 2.5% of the catalyst was observed

#### 4. Conclusions

The work reported here shows the good activity of ruthenium supported on alumina for the solvent-free selective oxidation of benzyl alcohol into benzaldehyde, i.e., a conversion of 62% and complete selectivity. The activity is related to the formation of metallic ruthenium nanoparticles on the support surface, and the higher the dispersion, the higher the activity. Furthermore, the catalyst was found to be very stable after several reaction cycles.

The proposed reaction follows the principles of green chemistry; indeed, no solvents were used, and the oxidant was air. The green chemistry metrics calculated for the AlRu-R indicated an environmentally friendly procedure (E-factor 0.51 and MP 66%), confirming the sustainability of the process. This is a preliminary study on the possibility of using heterogeneous catalysts for the oxidation of alcohols in more sustainable reaction conditions (compared with traditional reactions), and without the use of solvents. The next step of this work will be the optimization of the proposed catalytic formulations to improve the catalytic performance in terms of conversion.

**Supplementary Materials:** The following supporting information can be downloaded at: <https://www.mdpi.com/article/10.3390/inorganics11050177/s1>, Figure S1: Adsorption measurements. Table S1: TOF values. Figure S2: XPS spectra. Figure S3: Dependence of conversion of benzyl alcohol to benzaldehyde on ruthenium dispersion on the support. Figure S4: <sup>1</sup>H-NMR spectra.

**Author Contributions:** Conceptualization, E.A. and D.Z.; methodology, E.A. and D.Z.; investigation, E.A., F.C. and J.L.; data curation, E.A.; resources, W.B., A.T. and D.Z.; writing—original draft preparation, E.A.; writing—review and editing, E.A., W.B., J.L., A.T. and D.Z. All authors have read and agreed to the published version of the manuscript.

**Funding:** This research was funded by Projects MICINN/FEDER PID2021-124572OB-C31 and GC 2021 SGR 01061 (J.L.).

**Data Availability Statement:** The data presented in this study are available in the article and in the supplementary material.

**Acknowledgments:** J.L. is a Serra Hünter Fellow and is grateful to the ICREA Academia program.

**Conflicts of Interest:** The authors declare no conflict of interest.

#### References

1. Chan-Thaw, C.E.; Savara, A.; Villa, A. Selective Benzyl Alcohol Oxidation over Pd Catalysts. *Catalysts* **2018**, *8*, 431. [CrossRef]
2. Mallat, T.; Baiker, A. Oxidation of Alcohols with Molecular Oxygen on Solid Catalysts. *Chem. Rev.* **2004**, *104*, 3037–3058. [CrossRef]
3. Besson, M.; Gallezot, P. Selective oxidation of alcohols and aldehydes on metal catalysts. *Catal. Today* **2000**, *57*, 127–141. [CrossRef]
4. Najafshirtari, S.; Friedel Ortega, K.; Douthwaite, M.; Pattison, S.; Hutchings, G.J.; Bondue, C.J.; Tschulik, K.; Waffel, D.; Peng, B.; Deitermann, M.; et al. A Perspective on Heterogeneous Catalysts for the Selective Oxidation of Alcohols. *Chem. Eur. J.* **2021**, *27*, 16809–16833. [CrossRef] [PubMed]
5. Davis, S.E.; Ide, M.S.; Davis, R.J. Selective oxidation of alcohols and aldehydes over supported metal nanoparticles. *Green Chem.* **2013**, *15*, 17–45. [CrossRef]
6. Dhakshinamoorthy, A.; Asiri, A.M.; Garcia, H. Tuneable nature of metal organic frameworks as heterogeneous solid catalysts for alcohol oxidation. *Chem. Commun.* **2017**, *53*, 10851–10869. [CrossRef]
7. Sheldon, R.; Kochi, J. Activation of molecular oxygen by metal complexes. In *Metal-Catalyzed Oxidations of Organic Compounds*; Academic Press: New York, NY, USA, 1981.
8. Weng, Z.; Liao, G.; Wang, J.; Jian, X. Selective oxidation of benzyl alcohol with hydrogen peroxide over reaction-controlled phase-transfer catalyst. *Catal. Commun.* **2007**, *8*, 1493–1496. [CrossRef]

9. Schultz, M.J.; Sigman, M.S. Recent advances in homogeneous transition metal-catalyzed aerobic alcohol oxidations. *Tetrahedron* **2006**, *62*, 8227–8241. [[CrossRef](#)]
10. Vinod, C.P.; Wilson, K.; Lee, A.F. Recent advances in the heterogeneously catalysed aerobic selective oxidation of alcohols. *J. Chem. Technol. Biot.* **2011**, *86*, 161–171. [[CrossRef](#)]
11. Watanabe, H.; Asano, S.; Fujita, S.-I.; Yoshida, H.; Arai, M. Nitrogen-Doped, Metal-Free Activated Carbon Catalysts for Aerobic Oxidation of Alcohols. *ACS Catal.* **2015**, *5*, 2886–2894. [[CrossRef](#)]
12. Zhao, Y.; Yu, C.; Wu, S.; Zhang, W.; Xue, W.; Zeng, Z. Synthesis of Benzaldehyde and Benzoic Acid by Selective Oxidation of Benzyl Alcohol with Iron(III) Tosylate and Hydrogen Peroxide: A Solvent-Controlled Reaction. *Catal. Lett.* **2018**, *148*, 3082–3092. [[CrossRef](#)]
13. Shojaei, A.F.; Tabatabaieian, K.; Zanjanchi, M.A.; Moafi, H.F.; Modirpanah, N. Synthesis, characterization and study of catalytic activity of Silver doped ZnO nanocomposite as an efficient catalyst for selective oxidation of benzyl alcohol. *J. Chem. Sci.* **2015**, *127*, 481–491. [[CrossRef](#)]
14. Kunene, A.; Leteba, G.; van Steen, E. Liquid Phase Oxidation of Benzyl Alcohol over Pt and Pt–Ni Alloy Supported on TiO<sub>2</sub>: Using O<sub>2</sub> or H<sub>2</sub>O<sub>2</sub> as Oxidant? *Catal. Lett.* **2022**, *152*, 1760–1768. [[CrossRef](#)]
15. Göksu, H.; Burhan, H.; Mustafafov, S.D.; Şen, F. Oxidation of Benzyl Alcohol Compounds in the Presence of CarbonHybrid Supported Platinum Nanoparticles (Pt@CHs) in Oxygen Atmosphere. *Sci. Rep.* **2020**, *10*, 5439. [[CrossRef](#)]
16. Lukato, S.; Wendt, O.F.; Wallenberg, R.; Kasozi, G.N.; Naziriwo, B.; Persson, A.; Folkers, L.C.; Tebandeke, E. Selective oxidation of benzyl alcohols with molecular oxygen as the oxidant using Ag–Cu catalysts supported on polyoxometalates. *Results Chem.* **2021**, *3*, 100150. [[CrossRef](#)]
17. Chen, J.; Zhang, Q.; Wang, Y.; Wan, H. Size-Dependent Catalytic Activity of Supported Palladium Nanoparticles for Aerobic Oxidation of Alcohols. *Adv. Synth. Catal.* **2008**, *350*, 453–464. [[CrossRef](#)]
18. Nowicka, E.; Althahban, S.; Leah, T.D.; Shaw, G.; Morgan, D.; Kiely, C.J.; Roldan, A.; Hutchings, G.J. Benzyl alcohol oxidation with Pd–Zn/TiO<sub>2</sub>: Computational and experimental studies. *Sci. Technol. Adv. Mater.* **2019**, *20*, 367–378. [[CrossRef](#)] [[PubMed](#)]
19. Sankar, M.; He, Q.; Morad, M.; Pritchard, J.; Freakley, S.J.; Edwards, J.K.; Taylor, S.H.; Morgan, D.J.; Carley, A.F.; Knight, D.W.; et al. Synthesis of Stable Ligand-free Gold–Palladium Nanoparticles Using a Simple Excess Anion Method. *ACS Nano* **2012**, *6*, 6600–6613. [[CrossRef](#)] [[PubMed](#)]
20. Wu, P.; Cao, Y.; Zhao, L.; Wang, Y.; He, Z.; Xing, W.; Bai, P.; Mintova, S.; Yan, Z. Formation of PdO on Au–Pd bimetallic catalysts and the effect on benzyl alcohol oxidation. *J. Catal.* **2019**, *375*, 32–43. [[CrossRef](#)]
21. Li, X.; Feng, J.; Perdjon, M.; Oh, R.; Zhao, W.; Huang, X.; Liu, S. Investigations of supported Au–Pd nanoparticles on synthesized CeO<sub>2</sub> with different morphologies and application in solvent-free benzyl alcohol oxidation. *Appl. Surf. Sci.* **2020**, *505*, 144473. [[CrossRef](#)]
22. Liu, J.; Zou, S.; Wu, J.; Kobayashi, H.; Zhao, H.; Fan, J. Green catalytic oxidation of benzyl alcohol over Pt/ZnO in base-free aqueous medium at room temperature. *Chin. J. Catal.* **2018**, *39*, 1081–1089. [[CrossRef](#)]
23. Pagliaro, M.; Campestrini, S.; Ciriminna, R. Ru-based oxidation catalysis. *Chem. Soc. Rev.* **2005**, *34*, 837–845. [[CrossRef](#)]
24. Gore, E.S. Ruthenium Catalysed Oxidations of Organic Compounds. *Platin. Met. Rev.* **1983**, *27*, 111–125.
25. Griffith, W.P. The chemistry of ruthenium oxidation complexes. In *Ruthenium Oxidation Complexes: Their Uses as Homogenous Organic Catalysts*; Griffith, W.P., Ed.; Springer: Dordrecht, The Netherlands, 2011; pp. 1–134. [[CrossRef](#)]
26. Dey, S.; Dhal, G.C. Applications of Rhodium and Ruthenium Catalysts for CO Oxidation: An Overview. *Polytechnica* **2020**, *3*, 26–42. [[CrossRef](#)]
27. Kamdar, J.M.; Grotjahn, D.B. An Overview of Significant Achievements in Ruthenium-Based Molecular Water Oxidation Catalysis. *Molecules* **2019**, *24*, 494. [[CrossRef](#)] [[PubMed](#)]
28. Matarrese, R.; Aneggi, E.; Castoldi, L.; Llorca, J.; Trovarelli, A.; Lietti, L. Simultaneous removal of soot and NO<sub>x</sub> over K- and Ba-doped ruthenium supported catalysts. *Catal. Today* **2016**, *267*, 119–129. [[CrossRef](#)]
29. Zheng, C.; Mao, D.; Xu, Z.; Zheng, S. Strong Ru–CeO<sub>2</sub> interaction boosts catalytic activity and stability of Ru supported on CeO<sub>2</sub> nanocube for soot oxidation. *J. Catal.* **2022**, *411*, 122–134. [[CrossRef](#)]
30. Qin, X.; Chen, X.; Chen, M.; Zhang, J.; He, H.; Zhang, C. Highly efficient Ru/CeO<sub>2</sub> catalysts for formaldehyde oxidation at low temperature and the mechanistic study. *Catal. Sci. Technol.* **2021**, *11*, 1914–1921. [[CrossRef](#)]
31. Mao, J.X.; Jiang, J.; Wang, H.K.; Yang, L.J.; Wang, Y.N.; Geng, J.; Wang, X.Z.; Hu, Z. Immobilizing Ruthenium Nanoparticles onto Nitrogen-Doped Carbon Nanotubes for Aerobic Oxidation of Benzyl Alcohol under Ambient Pressure. *Chin. J. Inorg. Chem.* **2012**, *28*, 2508–2512.
32. Opre, Z.; Ferri, D.; Krumeich, F.; Mallat, T.; Baiker, A. Aerobic oxidation of alcohols by organically modified ruthenium hydroxyapatite. *J. Catal.* **2006**, *241*, 287–295. [[CrossRef](#)]
33. Shan, Y.Y.; Yu, C.; Zhang, X.; Zhang, M.D.; Dong, Q.; Qiu, J.S. Fabrication of a Ru–NiAl layered double hydroxide-oxidized CNT hybrid catalyst for the selective oxidation of benzyl alcohol to benzaldehyde. *New Carbon. Mater.* **2018**, *33*, 109–115.
34. Yang, X.M.; Wang, X.N.; Qiu, J.S. Aerobic oxidation of alcohols over carbon nanotube-supported Ru catalysts assembled at the interfaces of emulsion droplets. *Appl. Catal. A Gen.* **2010**, *382*, 131–137. [[CrossRef](#)]
35. Yasu-eda, T.; Kitamura, S.; Ikenaga, N.; Miyake, T.; Suzuki, T. Selective oxidation of alcohols with molecular oxygen over Ru/CaO–ZrO<sub>2</sub> catalyst. *J. Mol. Catal. A Chem.* **2010**, *323*, 7–15. [[CrossRef](#)]

36. Zadam, B.; Obaid, D.; Mayoufi, A.; Beaunier, P.; Launay, F.; El Berrichi, F.Z. Aerobic oxidation of alcohols using ruthenium supported on DD3 kaolin. *Res. Chem. Intermediat.* **2019**, *45*, 1281–1293. [[CrossRef](#)]
37. Yamaguchi, K.; Mizuno, N. Supported Ruthenium Catalyst for the Heterogeneous Oxidation of Alcohols with Molecular Oxygen. *Angew. Chem. Int. Ed.* **2002**, *41*, 4538–4542. [[CrossRef](#)]
38. Zhao, J.P.; Hernandez, W.Y.; Zhou, W.J.; Yang, Y.; Vovk, E.I.; Capron, M.; Ordonsky, V. Selective Oxidation of Alcohols to Carbonyl Compounds over Small Size Colloidal Ru Nanoparticles. *Chemcatchem* **2020**, *12*, 238–247. [[CrossRef](#)]
39. Goodman, D.W.; Peden, C.; Chen, M. CO oxidation on ruthenium: The nature of the active catalytic surface. *Surf. Sci.* **2007**, *601*, 54212. [[CrossRef](#)]
40. Ramirez-Barria, C.S.; Isaacs, M.; Parlett, C.; Wilson, K.; Guerrero-Ruiz, A.; Rodriguez-Ramos, I. Ru nanoparticles supported on N-doped reduced graphene oxide as valuable catalyst for the selective aerobic oxidation of benzyl alcohol. *Catal. Today* **2020**, *357*, 8–14. [[CrossRef](#)]
41. Nagy, G.; Gal, T.; Sranko, D.F.; Safran, G.; Maroti, B.; Sajo, I.E.; Schmidt, F.P.; Beck, A. Selective aerobic oxidation of benzyl alcohol on alumina supported Au-Ru and Au-Ir catalysts. *Mol. Catal.* **2020**, *492*, 110917. [[CrossRef](#)]
42. Aneggi, E.; Campagnolo, F.; Segato, J.; Zuccaccia, D.; Baratta, W.; Llorca, J.; Trovarelli, A. Solvent-free selective oxidation of benzyl alcohol using Ru loaded ceria-zirconia catalysts. *Mol. Catal.* **2023**, *540*, 113049. [[CrossRef](#)]
43. Clarke, C.J.; Tu, W.-C.; Levers, O.; Bröhl, A.; Hallett, J.P. Green and Sustainable Solvents in Chemical Processes. *Chem. Rev.* **2018**, *118*, 747–800. [[CrossRef](#)] [[PubMed](#)]
44. Anastas, P.T.; Allen, D.T. Twenty-Five Years of Green Chemistry and Green Engineering: The End of the Beginning. *ACS Sustain. Chem Eng* **2016**, *4*, 5820. [[CrossRef](#)]
45. Anastas, P.; Han, B.; Leitner, W.; Poliakov, M. “Happy silver anniversary”: Green Chemistry at 25. *Green Chem.* **2016**, *18*, 12–13. [[CrossRef](#)]
46. Hessel, V.; Tran, N.N.; Asrami, M.R.; Tran, Q.D.; Van Duc Long, N.; Escrivà-Gelonch, M.; Tejada, J.O.; Linke, S.; Sundmacher, K. Sustainability of green solvents—Review and perspective. *Green Chem.* **2022**, *24*, 410–437. [[CrossRef](#)]
47. Sheldon, R.A. Sustainable chemistry in practice. *Nat. Rev. Methods Prim.* **2022**, *2*, 61. [[CrossRef](#)]
48. Sheldon, R.A. Metrics of Green Chemistry and Sustainability: Past, Present, and Future. *ACS Sustain. Chem. Eng.* **2018**, *6*, 32–48. [[CrossRef](#)]
49. Constable, D.J.C.; Curzons, A.D.; Cunningham, V.L. Metrics to ‘green’ chemistry—Which are the best? *Green Chem.* **2002**, *4*, 521–527. [[CrossRef](#)]
50. Sheldon, R.A. The E factor 25 years on: The rise of green chemistry and sustainability. *Green Chem.* **2017**, *19*, 18–43. [[CrossRef](#)]
51. Mulvihill, M.J.; Beach, E.S.; Zimmerman, J.B.; Anastas, P.T. Green Chemistry and Green Engineering: A Framework for Sustainable Technology Development. *Annu. Rev. Environ. Resour.* **2011**, *36*, 271–293. [[CrossRef](#)]
52. Grunwaldt, J.-D.; Caravati, M.; Baiker, A. Oxidic or Metallic Palladium: Which Is the Active Phase in Pd-Catalyzed Aerobic Alcohol Oxidation? *J. Phys. Chem. B* **2006**, *110*, 25586–25589. [[CrossRef](#)]
53. Panagiotopoulou, P.; Verykios, X.E. Metal-support interactions of Ru-based catalysts under conditions of CO and CO<sub>2</sub> hydrogenation. In *Catalysis*; The Royal Society of Chemistry: London, UK, 2020; Volume 32, pp. 1–23.
54. Villani, K.; Kirschhock, C.E.A.; Liang, D.; Van Tendeloo, G.; Martens, J.A. Catalytic Carbon Oxidation Over Ruthenium-Based Catalysts. *Angew. Chem. Int. Ed.* **2006**, *45*, 3106–3109. [[CrossRef](#)] [[PubMed](#)]
55. Mishra, D.K.; Lee, H.J.; Kim, J.; Lee, H.-S.; Cho, J.K.; Suh, Y.-W.; Yi, Y.; Kim, Y.J. MnCo<sub>2</sub>O<sub>4</sub> spinel supported ruthenium catalyst for air-oxidation of HMF to FDCA under aqueous phase and base-free conditions. *Green Chem.* **2017**, *19*, 1619–1623. [[CrossRef](#)]
56. Barbier, J.; Delanoë, F.; Jabouille, F.; Duprez, D.; Blanchard, G.; Isnard, P. Total oxidation of acetic acid in aqueous solutions over noble metal catalysts. *J. Catal.* **1998**, *177*, 378–385. [[CrossRef](#)]
57. Ayusheev, A.B.; Taran, O.P.; Seryak, I.A.; Podyacheva, O.Y.; Descorme, C.; Besson, M.; Kibis, L.S.; Boronin, A.I.; Romanenko, A.I.; Ismagilov, Z.R.; et al. Ruthenium nanoparticles supported on nitrogen-doped carbon nanofibers for the catalytic wet air oxidation of phenol. *Appl. Catal. B Environ.* **2014**, *146*, 177–185. [[CrossRef](#)]
58. Poirier, M.G.; Trudel, J.; Guay, D. Partial oxidation of methane over ruthenium catalysts. *Catal. Lett.* **1993**, *21*, 99–111. [[CrossRef](#)]
59. Mitsui, T.; Tsutsui, K.; Matsui, T.; Kikuchi, R.; Eguchi, K. Support effect on complete oxidation of volatile organic compounds over Ru catalysts. *Appl. Catal. B Environ.* **2008**, *81*, 56–63. [[CrossRef](#)]
60. Yi, X.-T.; Li, C.-Y.; Wang, F.; Xu, J.; Xue, B. The solvent-free and aerobic oxidation of benzyl alcohol catalyzed by Pd supported on carbon nitride/CeO<sub>2</sub> composites. *New J. Chem.* **2022**, *46*, 7108–7117. [[CrossRef](#)]
61. Zhang, H.; Zheng, Z.; Ma, C.; Zheng, J.; Zhang, N.; Li, Y.; Chen, B.H. Tuning Surface Properties and Catalytic Performances of Pt–Ru Bimetallic Nanoparticles by Thermal Treatment. *Chemcatchem* **2015**, *7*, 245–249. [[CrossRef](#)]
62. Alsaiani, R.; Rizk, M.A.; Musa, E.; Alqahtani, H.; Alqadri, F.; Mohamed, M.; Alsaiani, M.; Alkorbi, A.; Shedaiwa, I.; Alkorbi, F. Supported Ruthenium Catalysts for Oxidation of Benzyl Alcohol under Solvent-Free Conditions. *J. Chem. Soc. Pak.* **2022**, *44*, 322–329. [[CrossRef](#)]
63. Jenkins, R.; Snyder, R.L. *Introduction to X-ray Powder Diffractometry*; Wiley: New York, NY, USA, 1996.

**Disclaimer/Publisher’s Note:** The statements, opinions and data contained in all publications are solely those of the individual author(s) and contributor(s) and not of MDPI and/or the editor(s). MDPI and/or the editor(s) disclaim responsibility for any injury to people or property resulting from any ideas, methods, instructions or products referred to in the content.